LCA Methodology

Expanded Damage Function of Stratospheric Ozone Depletion to Cover Major Endpoints Regarding Life Cycle Impact Assessment

Kentaro Hayashi[1]*, Ai Nakagawa[2], Norihiro Itsubo[3] and Atsushi Inaba[3]

[1] Department of Environmental Chemistry, National Institute for Agro-Environmental Sciences (NIAES), 3-1-3 Kan-nondai, Tsukuba, 305-8604, Japan
[2] Environmental Department, Pacific Consultants Co. Ltd., 2-7-1 Nishi-Shinjuku, Shinjuku, 163-0730, Japan
[3] Research Center for Life Cycle Assessment, National Institute of Advanced Industrial Science and Technology (AIST), 16-1 Onogawa, Tsukuba, 305-8569, Japan

* **Corresponding author** (kentaroh@affrc.go.jp)

DOI: http://dx.doi.org/10.1065/lca2004.11.189

Abstract

Background. Stratospheric ozone depletion is one of the important environmental issues for LCIA. The National LCA Project of Japan has developed a framework of LCIA since 1998, which tackles the issue employing an endpoint approach. Although the basic components were available in 2000, it was required that the target endpoints should be expanded in particular.

Objective. This study aimed at expanding the scope of damage function of ozone depletion in the LCIA framework of LIME. Damage function gives potential and quantitative damage for each endpoint per unit emission of ODS.

Methods. Marginal damage due to the unit emission of ODS was calculated for 13 substances for which quantitative information was available as follows: (1) the increase of UVB radiation at the earth's surface per unit emission of ODS was estimated, (2) the increase of potential damage per unit increase of UVB radiation was estimated, (3) the increase of potential damage per unit emission of ODS was determined by connecting the two relationships, and (4) correcting by the atmospheric lifetime of ODS, so that the damage function was then obtained. For other ODSs regulated by the Montreal Protocol, their damage functions were estimated by multiplying the ratio of ODP compared to the corresponding reference substance by the damage function of this reference substance.

Results and Discussion. The damage function of ozone depletion included the following endpoints: skin cancer and cataract for human health, crop production and timber production for social assets, and terrestrial NPP and aquatic NPP for primary productivity. And damage factors for each safeguard subject were also obtained.

Conclusion. The damage function of ozone depletion could cover all ODSs regulated by the Montreal Protocol and also cover important endpoints. Uncertainty of damage function is also an important point to be elucidated. Preliminary studies of uncertainty analysis have begun for the damage function of ozone depletion. However, further analysis is required to comprehensively evaluate the uncertainty of the damage function.

Keywords: Damage function; human health; life cycle impact assessment; ozone depleting substance; primary productivity; skin cancer; cataract; social assets; stratospheric ozone depletion; ultraviolet B

Abbreviations: BCC-Basal Cell Carcinoma; CFC-Chlorofluorocarbon; DALY-Disability Adjusted Life Years; DF-Damage Factor; DI-Damage Indicator; EESC-Equivalent Effective Stratospheric Chlorine; HBFC-Hydrobromofluorocarbon; HCFC-Hydrochlorofluorocarbon; LCA-Life Cycle Assessment; LCIA-Life Cycle Impact Assessment; LIME-Life-cycle Impact assessment Method based on Endpoint modeling; MM-malignant melanoma; NPP-Net Primary Production; ODP-Ozone Depletion Potential; ODS-Ozone Depleting Substance; SCC-Squamous Cell Carcinoma; TCL-Tropospheric Chlorine Loading; UVB-Ultraviolet B; YLD-Years of Life Disabled; YLL-Years of Life Lost

Introduction

Stratospheric ozone depletion caused by anthropogenic ODS emissions is one of the serious and imminent environmental threats to both the anthroposphere and the biosphere; it is also an important issue in LCIA. As mentioned in the previous paper (Hayashi et al. 2000), early LCIA studies tackled the issue mainly employing midpoint approaches with ODP (Solomon and Albritton 1992) as a characterization factor; ODP is a relative index denoting the ratio of ozone-depleting ability of certain ODSs to that of CFC-11, whereas there are a few endpoint approaches in LCIA that evaluate concrete damage induced by ozone depletion (e.g. Goedkoop and Spriensma 2000, Steen 1999). Under the circumstances, the LCA National Project of Japan developed LIME, a comprehensive methodology for LCIA also including endpoint approaches (Itsubo and Inaba 2003, Itsubo et al. 2004). The framework of LIME also has an endpoint approach for ozone depletion (**Fig. 1**). In the framework of LIME, damage function is defined as the quantitative relationship between an inventory of causative substances or activities and potential effects on each category endpoint. Moreover, a damage factor (DF) of certain impact categories is defined as the sum of damage function for individual safeguard subjects, i.e. human health, social assets, biodiversity, and primary productivity.

The previous paper (Hayashi et al. 2000) reported the basic component of the damage function of ozone depletion, though it was under development at the time. The revised framework is briefly presented in Hayashi et al. (2002). This subsequent paper aims to describe the more expanded frame-

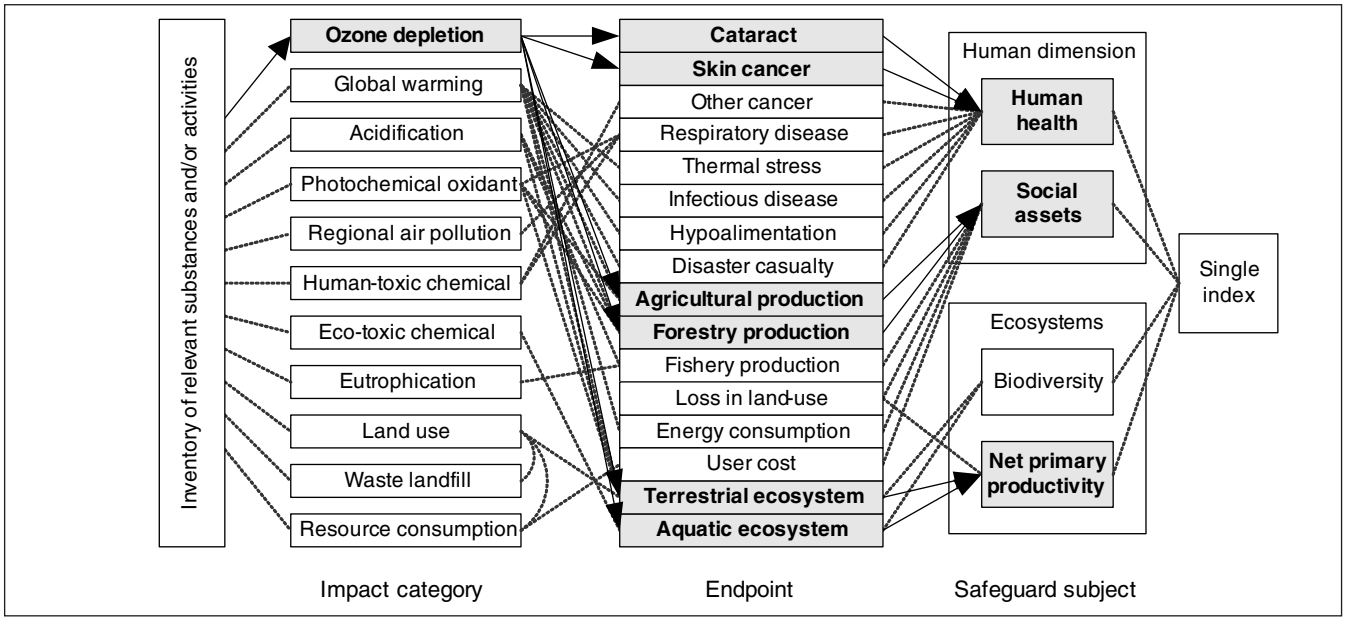

Fig. 1: LCIA framework of LIME with emphasis on the category of ozone depletion

work of the damage function of ozone depletion in LIME. It should be noted that there is a large difference in quality and quantity of available information among endpoints. Therefore, a determination of damage function for an endpoint lacking in relevant information involves a large degree of uncertainty. However, this study attached importance to cover all endpoints regarding ozone depletion because of completing the coverage of LIME.

1 Method

1.1 Target ODSs

There are a number of chemical species that have ozone depleting ability, i.e. ODSs most of which are artificial. Quantitative information such as atmospheric life time is required to calculate a damage function. Therefore, it was practically impossible to determine a damage function for all ODSs because of the paucity of quantitative information. The damage function of ozone depletion could be directly determined for 13 ODS species in LIME (**Table 1**).

Furthermore, the damage function of ozone depletion for other ODSs was indirectly calculated to cover all ODSs under the regulation of the Montreal Protocol. The ODP ratio of a target substance to a reference substance was applied to the indirect calculation,

$$damage\ function(X) = damage\ function(R) \cdot ODP(X) / ODP(R) \quad (1)$$

where subscripts X and R denote a target substance and a reference substance, respectively. The selected reference substances were as follows: CFC-11 for CFCs, Halon-1211 for Halons, and HCFC-22 for HCFCs and HBFCs. The values of ODP were established according to the Montreal Protocol. The maximum value of ODPs was chosen for a chemical species with structural isomers.

1.2 Cause of damage

The most important change induced by ozone depletion is an increase of UVB at the earth's surface (UNEP 1998). There are two definitions of UVB wavelength range, i.e. 280–315 nm (CIE 1987) in illumination engineering and meteorology, and 290–320 nm (Sasaki et al. 1993) in photobiology. LIME adopted the UVB wavelength range of 290–320 nm to obtain the damage function of ozone depletion, because ultraviolet radiation of less than 290 nm hardly reaches the earth's surface (Jendritzky 1997, JMA 1998). The increase of UVB brings about adverse effects on wide-ranging endpoints (**Table 2**). Table 2 also shows whether LIME evaluated the respective endpoints or not.

Table 1: ODSs with direct calculation of damage function of ozone depletion in LIME

Group	No. of substance	Name of substance
CFC	3	CFC-11, CFC-12, CFC-113
Halon	2	Halon-1211, Halon-1301
HCFC	5	HCFC-22, HCFC-123, HCFC-124, HCFC-141b, HCFC-142b
Chlorocarbon	2	Carbon tetrachloride (CCl_4), 1,1,1-trichloroethane (1,1,1-TCE)
Bromocarbon	1	Methyl bromide (CH_3Br)

Table 2: Major endpoints relevant to ozone depletion and its inclusion in LIME

Major division	Minor division	Endpoint relevant to UVB exposure	Inclusion In LIME
Human health	Skin	Skin cancer (malignant melanoma, basal cell carcinoma, and squamous cell carcinoma)	Yes
		Other disorders (solar keratosis and photo-aging)	No
	Eye	Cataract (cortex type and nuclei type)	Yes
		Other disorders (pterygium and corneal disorders)	No
	Immune	Immunosuppression	No
Social Assets	Crops	Diminution in production	Yes
		Other aspects such as quality	No
	Timbers	Diminution in production	Yes
		Other aspects such as quality	No
	Materials	Degradation and deterioration	No
Biodiversity	Terrene	Interspecies competition due to differences in UVB susceptibility	No
	Aqua	Interspecies competition due to differences in UVB susceptibility	No
Net primary productivity	Terrene	Primary productivity of coniferous forests	Yes
		Primary productivity of other terrestrial vegetation	No
	Aqua	Primary productivity of phytoplankton (high latitudes)	Yes
		Primary productivity of phytoplankton (middle and low latitudes)	No
General circulation of the atmosphere		Climate due changes in atmospheric chemistry and heat budget	No

1.3 Revised methodological framework

LIME addresses it as damage to be evaluated, i.e. an increment of damage due to an additional ODS emission given by inventory, or so-called marginal damage. For example, the damage function for cataract gives a potential increase of cataract incidence to 1 kg yr^{-1} emission of CFC-11. **Fig. 2** shows the framework of damage function of ozone depletion; a brief description is as follows: (1) the increase of UVB radiation at the earth's surface per unit emission of ODS compared to that of the benchmark year was estimated, (2) the increase of potential damage per unit increase of UVB radiation was estimated, (3) the increase of potential dam-

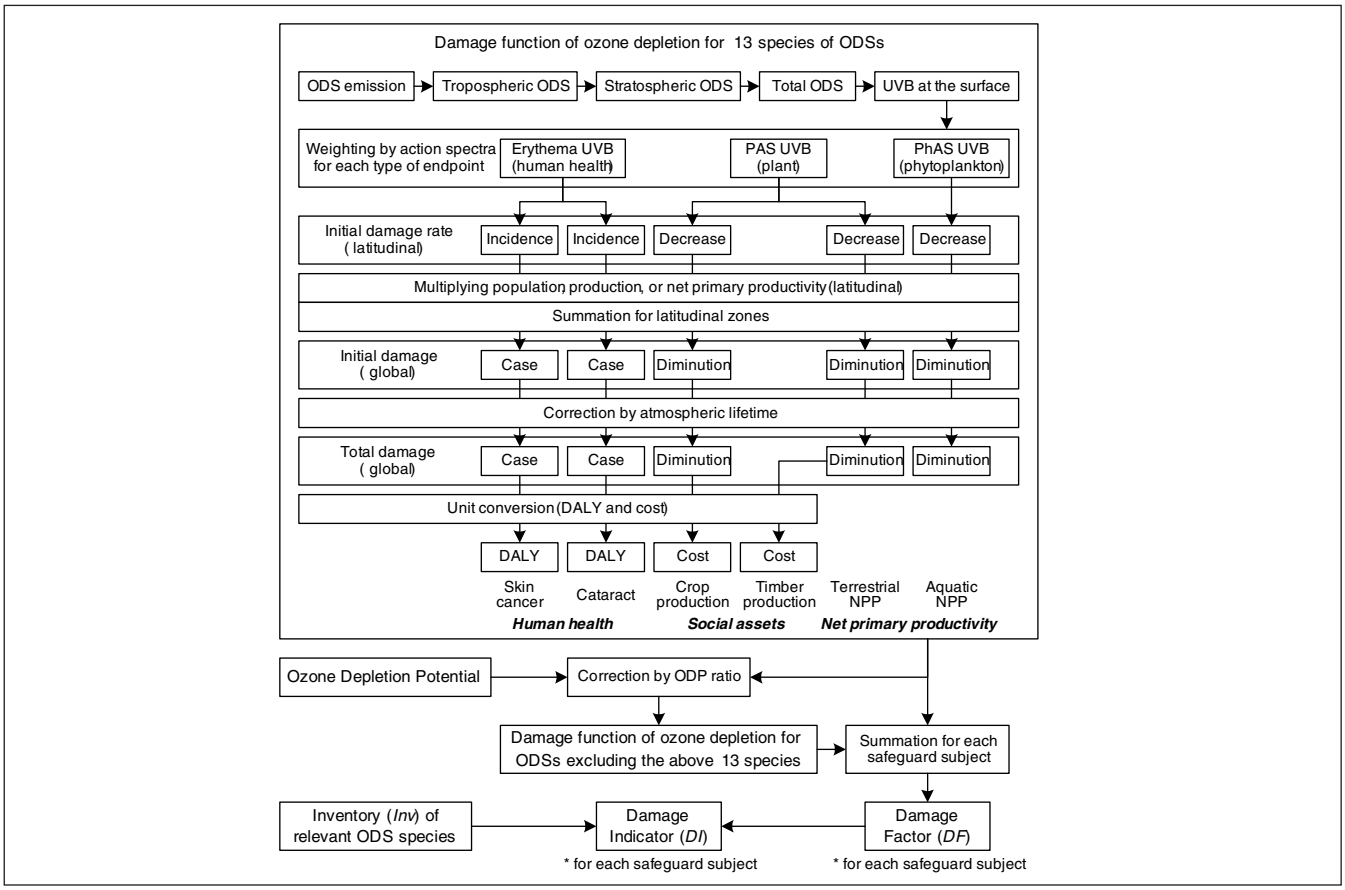

Fig. 2: Schematic diagram of the damage function of ozone depletion

age per unit emission of ODS was derived using the above two relationships, and (4) correcting by the atmospheric lifetime of ODS, so that damage function was then obtained. The benchmark year was set in 1998. The methodological framework is basically the same as shown in Hayashi et al. (2000). However, the following improvements were performed: (1) all ODSs under the control of the Montreal Protocol were targeted to derive their damage function; (2) polar zones were also included to estimate induced damage; (3) endpoints were expanded to cover the major endpoints regarding ozone depletion (see Table 2); and (4) the wavelength dependency of UVB action to each type of endpoint was included.

1.4 Relationship between ODS emission and UVB increase

1.4.1 ODS emission and its concentration in the troposphere

TCL (Daniel et al. 1995), an equivalent concentration on the basis of chlorine content, was applied to express a concentration of ODS in the troposphere. TCL was assumed to be globally homogeneous. The relationship between an annual global emission of CFC-11 (Kaye et al. 1994) and a concentration of TCL was linearly regressed (Hayashi et al. 2000). The slope of regression, $F_{TCL}(CFC11)$, was applied to calculate an increase of CFC-11 concentration in the troposphere to a unit emission of CFC-11. The following modification was applied to the other 12 species,

$$F_{TCL}(X) = 45.8 \cdot \frac{nCl(X) + nBr(X) \cdot \alpha}{MW(X)} \cdot F_{TCL}(CFC11) \qquad (2)$$

where X denotes certain ODS species, nCl and nBr the number of chlorine and bromine atom per molecule of X, respectively, α the ratio of ozone depleting activity of bromine to that of chlorine, i.e. 40-fold (WMO 1995), and MW the molecular weight of X.

1.4.2 ODS concentration in the troposphere and stratosphere

EESC (Daniel et al. 1995), an equivalent concentration on the basis of the fraction of chlorine release that causes ozone destruction, was applied to express a concentration of ODS in the stratosphere. EESC, also assumed to be globally homogeneous, was calculated as follows:

$$EESC(X,t) = \sum_{X} TCL(X, t-3) \cdot FC(X) \qquad (3)$$

where t denotes time (yr). Three years of delay in TCL to EESC means that it takes an average of 3 years for ODS transportation from the troposphere to the stratosphere (WMO 1995). FC denotes fractional chlorine release (Daniel et al. 1995), the values of which were determined as shown in Hayashi et al. (2000).

1.4.3 ODS concentration in the stratosphere and total ozone

Total ozone, equal to column ozone, expresses the total ozone amount integrated from the earth's surface to the top of the atmosphere. Total ozone approximates the stratospheric ozone, because 90% of ozone exists in the stratosphere (WMO 1999). A group of linear models was obtained by relating the temporal trend of total ozone by satellite observation (MacPeter and Beach 1996), since the objective variable with the temporal trend of total EESC by numerical simulation (WMO 1999) was employed as the explanatory variable. These linear models were prepared for each latitudinal zone with 10 degrees of width and season, i.e. March to May, June to August, September to November and December to February; however, the latitudinal zones in the season of polar night were excluded from the linear models. The concentrations of stratospheric ozone have a spatial distribution with a meridian gradient and these vary seasonally (WMO 1995). An example of the correlation is shown in Hayashi et al. (2000).

1.4.4 Total ozone and UVB intensity at the surface

The relationship between an apparent optical thickness, τ_{app}, as the objective variable and a theoretical optical thickness of ozone to UVB, τo_3, as the explanatory variable for each UVB wavelength band, 290–300, 300–310, and 310–320 nm, was linearly related with the observation in Japan in 1995 (Hayashi et al. 2000). τo_3 that expresses the optical thickness to direct UVB radiation is a function of total ozone; a molecule of ozone has a known cross section of absorption to UVB (Houghton 1986). Meanwhile, τ_{app} that approximates a combined optical thickness to direct and scattered UVB radiation was estimated here using Lambert-Beer's law, with the observation of UVB radiation at the earth's surface, solar zenith angle, and total ozone. Thus, the UVB intensity at the earth's surface to any total ozone and any solar zenith angle can be approximated by

$$I_{\lambda_1-\lambda_2} = I_{0\,\lambda_1-\lambda_2} \cdot \exp\left(-\tau_{app\,\lambda_1-\lambda_2} / \cos ZA\right) \qquad (4)$$

where I denotes the UVB intensity at the earth's surface (W m^{-2}), I_0 the UVB intensity at the top of the atmosphere (W m^{-2}) equal to the corresponding component of the solar constant (Houghton 1986), ZA solar zenith angle (rad), and suffix $\lambda_1-\lambda_2$ a certain wavelength band.

1.4.5 Annual UVB increase and weighting by action spectra

Annual UVB at the earth's surface (J m^{-2} yr^{-1}) in each latitudinal zone in 1998, excluding the effects of clouds, was calculated as follows: (1) the seasonal mean of daily UVB for each wavelength band was calculated, (2) the seasonal UVB was derived from multiplying the daily UVB by the number of days in the corresponding season, and (3) the annual UVB was obtained as the sum of the seasonal UVB. The diurnal change of solar zenith angle was considered to calculate the daily UVB, because UVB intensity at the earth's surface is intensively influenced by the optical air mass, i.e. in proportion to the cosine of solar zenith angle. Namely, the daily UVB was obtained by multiplying the daytime length by the mean UVB intensity within the half-day (rad), H, corresponding to the hour angle from sunrise to noon or from noon to sunset. The mean UVB intensity was derived by averaging the UVB intensity at 11 points of daytime h (rad) = 0, 0.1H, 0.2H, ···, H.; Eq. 4 was used for calculating the UVB intensity. h = 0 and h = H correspond to noon and sunset, respectively. H is given by (Liou 2002),

$$H = \arccos(-\tan\phi \tan\delta) \qquad (5)$$

where φ and δ denotes the latitude of a target point (rad) and the solar declination (rad) given as a function of date. However, H was fixed as 12 hours in the white night and 0 hours in the polar night. The value of cosZA at any daytime h is expressed by (Liu 2002),

$$\cos ZA = \sin\phi \sin\delta + \cos\phi \cos\delta \cos h \quad (6)$$

The value of UVB determined herewith was physical quantity. It is known that there is a specific wavelength dependency on the action of UVB to organisms. In LIME, these dependencies were divided into three types of endpoints, human health, terrestrial plant, and phytoplankton, and were grasped by the following sources: CIE (1987) for human health, Caldwell (1971) for terrestrial plant, and Behrenfeld et al. (1993a) for phytoplankton (**Fig. 3**). The reference wavelengths were 298 nm for human health and 300 nm for flora. The average of the relative strength of the UVB action was calculated for each wavelength band to be used as the weighting coefficient for the wavelength dependency. An annual UVB weighted by the action spectra was derived from multiplying the physical UVB by the corresponding weighting coefficient, i.e. erythema (Ery-UVB) for human health, plant action spectra (PAS-UVB) for terrestrial plant, and phytoplankton action spectra (PhAS-UVB) for phytoplankton.

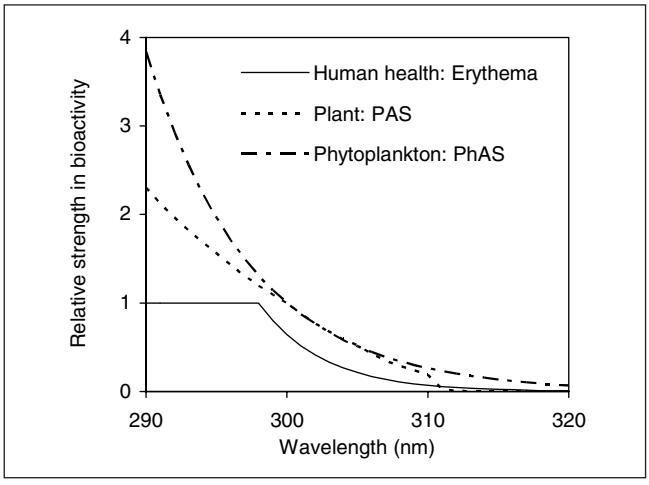

Fig. 3: UVB action spectra for each type of endpoint, human health (CIE 1987), plant (Caldwell 1971), and phytoplankton (Behrenfeld et al. 1993a). Reference wavelengths are 298 nm for human health and 300 nm for the others

1.4.6 UVB increase factor

Annual weighted-UVB in each latitudinal zone to a given additional emission of ODS can be calculated using the relationships as mentioned above. The increases of weighted-UVB in each latitudinal zone for 0, 100, 200, and 500 kt yr^{-1} of additional-global emissions of certain ODS showed a strong linearity for all ODS species (**Fig. 4**). Hence, the slope of the line was adopted as a factor, F_{UVBI} (X, i, E), that gives an increase of annual-weighted UVB for endpoint E, i.e., *Ery*, *PAS*, or *PhAS*, in latitudinal zone i to a unit emission of ODS X.

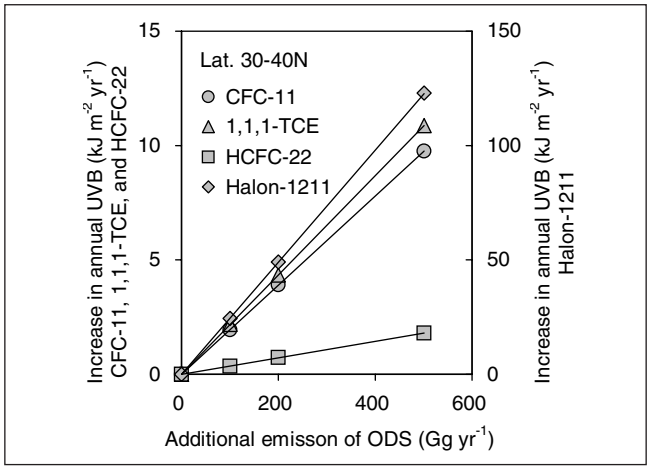

Fig. 4: An example of the relationships between given ODS emissions and estimated values of annual UVB at the earth's surface

1.5 Correction by atmospheric lifetime

Emitted ODS stays in the atmosphere generally more than 1 year. And the concentration of additionally emitted ODS at a certain time point decreases with time. Therefore, correction by atmospheric lifetime (WMO 1999) was needed to estimate the total damage due to an additional emission of ODS during its residence in the atmosphere. The fundamental concept of the correction is that damage at a certain time point is in proportion to the normalized concentration at the time, i.e. equal to 1 at the time of emission and 0 after the complete removal from the atmosphere. An exponential function was applied to express the decrease of ODS concentration in the atmosphere. And then, the integral of the exponential function was adopted as the correction coefficient of atmospheric lifetime, F_{LT}, that indicates the ratio of total damage to initial damage.

$$F_{LT}(X) = \int_3^\infty C(X,t)\,dt = \int_3^\infty e^{-t/LT(X)}\,dt \quad (7)$$

where $C(X, t)$ and $LT(X)$ denote normalized atmospheric concentration (dimensionless) of X at time t (yr) and atmospheric lifetime (yr) of X, respectively. Three years at the start of the integral means that it was assumed to take 3 years to transport ODS into the stratosphere (WMO 1995). Thus, the total damage could be derived from multiplying the initial damage due to a unit emission of X by $F_{LT}(X)$.

1.6 Impact on human health

1.6.1 Skin cancer

The relationship between annual UVB and skin cancer incidence shown in the previous paper (Hayashi et al. 2000) was revised by using erythema UVB to be related with skin cancer incidence, and adopting other data for the white race that was obtained from an epidemiological study of skin cancer incidence in Australia (Armstrong 1993). Meanwhile, similar to the previous paper (Hayashi et al. 2000), the statistic data of cancer incidence in the world (Ferlay et al. 1997) was applied to estimate the relationship between annual Ery-UVB and skin cancer incidence for yellow and black races. The Australian data classifies skin cancer into three

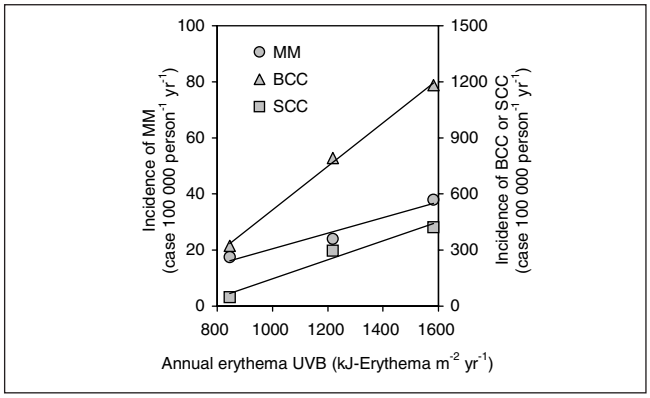

Fig. 5: Relationships between skin cancer incidence of the white race in Australia and annual erythema UVB

types, MM, BCC, and SCC, while the world data classifies it into two types, MM and non-melanoma skin cancer.

A linear model for each combination of skin color and skin cancer was derived from the statistic data; the objective variable was skin cancer incidence and the explanatory variable was annual Ery-UVB in 1998 at the location where the statistic data was obtained. The latter was calculated using the method mentioned in section 1.4. For the data of cancer incidence in the world, the correction of altitude that affects UVB attenuation was performed in order to calculate annual erythema UVB by multiplying the corresponding correction coefficient by the mean altitude of each country or region; the correction coefficients were classified into 5 altitude classes, 0–500, 500–1500, 1500–2500, 2500–3500, and over 3000 m. The slope of the linear model, F_{SCI}, was adopted as a coefficient that gives an increase of skin cancer incidence per unit increase of annual erythema UVB (case 100 000 person^{-1} J-erythema^{-1}) (**Fig. 5**).

The global and total damage of skin cancer per unit emission of ODS (case kg^{-1} yr), SCI_{global}, was then expressed by

$$SCI_{global}(X) = F_{LT}(X) \cdot \sum_i \sum_j F_{UVBI}(X, i, Ery) \cdot F_{SCI}(j) \cdot Pop(i, j) \quad (8)$$

where i and j denote latitudinal zone and skin color, respectively. $Pop(i, j)$ population of each skin color in each latitudinal zone (100 000 person) that was estimated using population statistics (UN 1998).

SCI_{global} was finally converted into DALY (Murray and Lopez 1996) in order to obtain damage function for skin cancer (DALY kg^{-1} yr). The value of DALY to a disease is expressed as the sum of YLL per death multiplied by its mortality and YLD per case; the value of YLD is determined by combining the duration of the disease and its disability weight. DALY of skin cancer was calculated referring to Godekoop and Spriensma (2000), thus 5.9, 0.88, and 0.29 DALY were obtained per case of MM, BCC, and SCC, respectively. Epidemiological data of the composition ratio of BCC and SCC, 86.5 and 13.5%, respectively (Dourmishev et al. 1997), was applied to estimate the averaged DALY of non-melanoma skin cancer, i.e. BCC and SCC, and then 0.34 DALY per case of non-melanoma skin cancer was obtained.

1.6.2 Cataract

In LIME, cataract was defined as eye lens opacity of grade II and over (Ono 2002), that inflicts an obstacle in daily life. An epidemiological study of cataract prevalence per age-group (Sasaki et al. 1997) was applied to estimate cataract incidence, because relevant information on incidence itself was absent. The study of Sasaki et al. (1997) covers four areas from low latitudes to high latitudes, i.e. Singapore, two areas in Japan, and Iceland; it was helpful to estimate the relationship between annual Ery-UVB and cataract incidence.

The cataract prevalence per each age group of fifties, sixties, and seventies was set at the center of each age group, e.g. 54.5 for fifties. Using this data plot, the logistic model with the maximum value of 100% was fitted for each area (**Fig. 6**). It was inferred that the age group of forties and over have the risk of cataract incidence according to the line shapes. Moreover, both the same mortality regardless of with or without cataract, and the same cataract incidence regardless of life and death per year, were presumed. The differential function of the logistic model, therefore, was adopted as a function that gives cataract incidence at any age. The cataract incidence for each age was then converted into the rate in population (case 100 000 person^{-1} yr^{-1}) using the world standard population by age group (Ferlay et al. 1997). A linear model with cataract incidence as the objective variable and annual Ery-UVB in 1998 as the explanatory variable was then derived. The latter was calculated using the method mentioned in section 1.4. The slope of linear model, F_{CATI}, was adopted as a coefficient that gives an increase of cataract incidence per unit increase of annual Ery-UVB (case 100 000 person^{-1} J-erythema^{-1}) (**Fig. 7**).

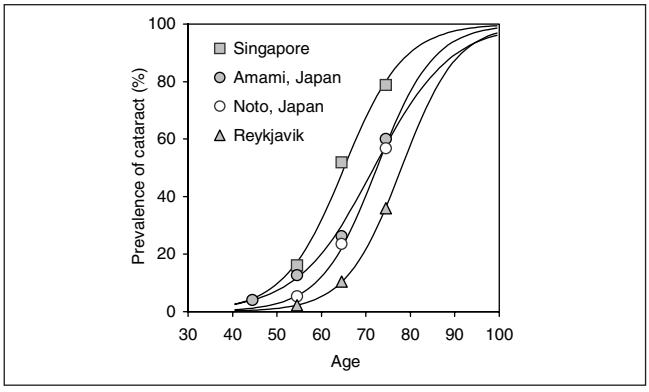

Fig. 6: Relationships between prevalence ratio of cataract and age in four regions

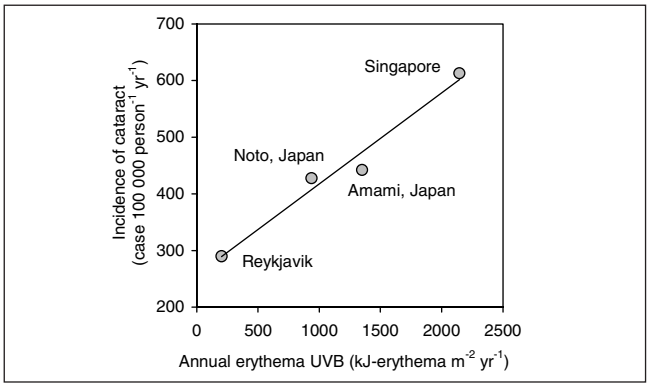

Fig. 7: Relationship between cataract incidence and annual erythema UVB

The global damage of cataract per unit emission of ODS (case kg^{-1} yr), $CATI_{global}$, was then expressed by

$$CATI_{global}(X) = F_{LT}(X) \cdot \sum_i F_{UVBI}(X, i, Ery) \cdot F_{CATI} \cdot Pop(i) \quad (9)$$

$CATI_{global}$ was finally converted into DALY to obtain damage function of cataract (DALY kg^{-1} yr). DALY of cataract was calculated using the same method as for skin cancer; 1.2 DALY per incidence was obtained.

1.7 Impact on primary productivity

1.7.1 Terrestrial ecosystems

Forest vegetation is the principal provider of terrestrial NPP. Although many studies of UVB effects on trees exist, quantitative information relevant to the relationship of plant growth to UVB exposure was quite limited; only several studies with seedlings of *Pinus taeda* (loblolly pine) (Sullivan and Teramura 1992, Naidu et al. 1993) were available. LIME adopted these data to estimate the relationship between an annual increase of PAS-UVB radiation and an annual decrease of growth rate as dry matter. The available information was that (1) 15–20% decrease in the biomass to control due to 3 years exposure of ultraviolet radiation corresponding to 25% decrease in stratospheric ozone (Sullivan and Teramura 1992), and (2) 24, 16, and 18% decreases in the biomass of root, stem, and foliage, respectively, to control due to the similar experimental conditions (Naidu et al. 1993). Then, the mean values of –17.5% for (1) and –19.3% for (2) were obtained. Annual PAS-UVB in 1998 and that corresponding to a 25% decrease of total ozone were calculated using the method mentioned in section 1.4, assuming that these experiments were done in the latitudinal zone of lat. 30–40°N. The mean decrease in the rate of plant growth per unit increase of PAS-UVB, F_{PGDR}, estimated to –0.0193% kJ-PAS^{-1} m^2 yr, was derived from averaging these values for (1) and (2). Loblolly pine is a coniferous species that is mainly distributed in the lowlands of southeastern USA. Such a lowlander is relatively susceptible to UVB exposure, while alpine tree species are generally tolerant to UVB exposure (Kossuth and Biggs 1981). Hence, the damage function for terrestrial NPP was aimed at coniferous forests excluding alpine-coniferous forests. The legends corresponding to these forests were extracted from a global vegetation dataset with 1° × 1° resolution (Matthews 1983), and the area of the forests in each latitudinal zone was summed. The sum, 35.5×10^6 km^2, that was three-fold that of the area of boreal forests of 12.0×10^6 km^2 (Matthews 1983), was taken as the sum of the areas of the boreal forests and other lowland-coniferous forests. The basic value of NPP was set to be constant as the average of boreal forests, 8000 kg ha^{-1} yr^{-1} (Whittaker 1975). The total NPP in each latitudinal zone (kg yr^{-1}), $NPP_{tr}(i)$, was obtained by multiplying the area of coniferous forests in i by the NPP of that. The global damage of terrestrial NPP per unit emission of ODS (kg kg^{-1} yr), $NPPD_{tr\ global}$, was then expressed by

$$NPPD_{tr\ global}(X) = F_{LT}(X) \cdot \sum_i F_{UVBI}(X, i, PAS) \cdot F_{PGDR} \cdot NPP_{tr}(i) \cdot 10^{-2} \quad (10)$$

1.7.2 Aquatic ecosystems

Phytoplankton is the principal provider of aquatic NPP. In spite of the rapid attenuation of UVB in the surface water, UVB has a potential of causing harmful effects on phytoplankton. Phytoplankton population mainly concentrates in the surface water to earn sunlight for photosynthesis, where UVB radiation can also reach. Therefore, damage function for aquatic NPP was introduced by considering the UVB attenuation in the surface water.

NPP of phytoplankton (kg m^{-2} yr^{-1}), NPP_{aq}, is expressed by

$$NPP_{aq} = (1-R) \cdot EC_C^{-1} \cdot C_{fix} \quad (11)$$

where R denotes the respiration ratio of photosynthesized carbon, 0.4 (Nielsen 1960), EC_C carbon composition of phytoplankton as dry matter, 0.359 (Redfield et al. 1963), and C_{fix} carbon fixation rate (kgC m^{-2} yr^{-1}). C_{fix} is given by

$$C_{fix} = C^u_{fix} \cdot D \cdot Z_0 \cdot 10^{-6} \quad (12)$$

where C^u_{fix} denotes carbon fixation rate per unit weight of chlorophyll-a (mgC mg^{-1} yr^{-1}), D chlorophyll-a density in the surface water (mg m^{-3}), and Z_0 water depth with UVB impact (m). It was assumed that D was constant within Z_0, that was considered to be the inverse of an extinction coefficient, k (m^{-1}). The value of k was given by an empirical equation at wavelength 305 nm, $k = 0.7\ D$ (Taguchi et al. 1994). Therefore, $D\ Z_0$ in Eq. (12) became the constant value, 1.43. On the other hand, C^u_{fix} was expressed by an empirical equation derived from the relationship between UVB dose and photosynthetic rate of marine phytoplankton in high latitudes (Behrenfeld et al. 1993a), namely,

$$C^u_{fix} = (1 - 0.000116\ UVB_{PhAS}) \cdot C^{u0}_{fix} \quad (13)$$

where C^{u0}_{fix} denotes the daily carbon fixation rate per unit weight of chlorophyll-a without UVB exposure (mgC mg^{-1} day^{-1}), expressed by Eq. (14) (Behrenfeld et al. 1993b), and UVB_{PhAS} the daily exposure of PhAS-UVB (J-PhAS m^{-2} day^{-1}), expressed by Eq. (15),

$$C^{u0}_{fix} = 2.87 \cdot h_{day} \quad (14)$$

$$UVB_{PhAS}(z) = UVB_{PhAS}(0) \cdot e^{-k\,z} \quad (15)$$

where h_{day} denotes day length (hours), z water depth (m). h_{day} is given by $48\ H/\pi$. Here, the water depth (m), Z', that equally divides the integrated UVB intensity from the water surface, i.e. $z = 0$, to the water depth of Z_0 was defined. Z' is expressed by

$$Z' = \frac{1}{k} \ln\left(1 + \frac{1}{2e}\right) \quad (16)$$

Inserting Z' into Eq. (15) as z, we obtain,

$$UVB_{PhAS}(Z') = \frac{2e}{2e+1} UVB_{PhAS}(0) \quad (17)$$

Using Eq. (11)–(14), and Eq. (17), the global damage of aquatic NPP per unit emission of ODS (kg kg^{-1} yr), $NPPD_{global}$, was then expressed by

$$NPPD_{aq}(X,i) = \sum_i \sum_s 3.683 \cdot A(i) \cdot Day(s) \cdot H(i,s) \cdot F_{UVBI}(X,i,s,PhAS) \cdot 10^{-9} \quad (18)$$

where s denotes season, $A(i)$ area of aquatic zone in i (m^2) determined by using the dataset of satellite observation (GSFC 2000), $Days(s)$ the number of days in s. Unlike the other endpoints, the damage of aquatic NPP was calculated for each season, i.e. seasonal damage per seasonal increase of PhAS-UVB radiation, and then summed up to the annual damage. It was to consider the seasonal change in photosynthesis. Moreover, i was limited here to the latitudinal zones north of lat. 50°N or south of lat. 50°S. Because Eq. (13) was derived from the experiments using phytoplankton in high latitudes with the correspondingly low UVB exposure in such regions (Behrenfeld et al. 1993a), the applicable range of UVB_{PhAS} of Eq. (13) was smaller than the daily UVB in mid and low latitudes. However, it was considered that an increase of UVB induced by ozone depletion is significant in high latitudes in particular, and then the damage of aquatic NPP mainly occurs in high latitudes. Hence, LIME adopted the damage function for aquatic NPP that was limited to high latitudes.

1.8 Impact on social assets

1.8.1 Crop production

Although there is a plenty of studies of UVB impact on crops (Krupa and Kickert 1989), quantitative information on adverse effects of UVB on crops was quite limited. In this situation, UNEP (1998) shows the compiled information of 49 relevant experiments on the relative changes of crop yields due to UVB exposure; the crop species are soy bean, rice, peas, and mustard. The average of changes in yield for each crop (%) that was read from the graph was –3.7 for soy bean (n = 29), –1.4 for rice (n = 14), –11.0 for peas (n = 4), and –19.5 for mustard (n = 2). It is reported that, although the experimental conditions were different for each case, the experiments generally corresponded to the 20% decrease of stratospheric ozone. Based on the assumption that these experiments were conducted in the latitudinal zone of lat. 30–40°N, the annual PAS-UVB in 1998 and that corresponding to the 20% decrease of total ozone were calculated using the method mentioned in section 1.4. Subsequently, the decrease rate of crop yield per unit increase of PAS-UVB for each crop species (% kJ-PAS^{-1} m^2), F_{CYDR}, was obtained. A statistical database, FAOSTAT (FAO 2000), was used to grasp the production of crop species m in each country in 1998. And then, the total production in each latitudinal zone (kg yr^{-1}), $CP(i, m)$, was estimated. The global damage of crop production per unit emission of ODS (kg kg^{-1} yr), CPD_{global}, was then expressed by

$$CPD_{global}(m,X) = F_{LT}(X) \cdot \sum_i \sum_m F_{UVBI}(X,i,PAS) \cdot F_{CYDR}(m) \cdot CP(i,m) \quad (19)$$

CPD_{global} was finally converted into money to obtain a damage function for crop production (yen kg^{-1} yr). Yen equivalent of unit producer cost was estimated at 240, 243, 550, 30 yen kg^{-1} yr for soy, rice, peas, and mustard, respectively, based on the relevant statistics (FAO 2000, MAFF 2002a).

1.8.2 Timber production

Damage of terrestrial NPP as a primary productivity simultaneously becomes a damage of timber production as social assets. It was assumed that damage of terrestrial NPP is directly applicable to the damage of timber production, because of the damage function for terrestrial NPP-targeted coniferous forests that are useful as timber resources. Unit producer costs of timber for saw, woodchip, and pulp in Japan (yen m^{-3}) were arithmetically averaged and converted into the mass basis (yen kg^{-1} yr) with a mean density of timber of 500 kg m^{-3}. The damage function of terrestrial NPP was converted into money using the mass basis unit of cost (MAFF 2002b) to obtain a damage function for timber production.

2 Results

2.1 Damage function and damage factor of stratospheric ozone depletion

Table 3 shows the derived damage function of ozone depletion for each endpoint; however, it is noted that Table 3 shows the damage function for 13 ODS species with direct calculation. Comparing the values of damage function among ODSs species, the values were high for Halons which contain bromine and have relatively long atmospheric lifetimes, and were low for HCFCs which have short atmospheric lifetimes. On the other hand, comparing them within each safeguard subject, the damage function of skin cancer was similar to that of cataract. The relatively lower risk and the higher DALY for skin cancer were comparable to the inverse features for cataract. The damage function of aquatic NPP was about double-digits larger than that of terrestrial NPP because of the higher sensitivity of aquatic NPP to UVB and the larger area of coverage. The damage function of timber production was tenfold larger than the total of the damage function of crop production because of the higher sensitivity of terrestrial NPP which expresses the sensitivity of timber production.

The damage factor that indicates the total damage for each safeguard subject per unit emission of ODS, DF, also shown in Table 3, is expressed by

$$DF(X,SS) = \sum_{EP} damage\ function(X,EP,SS) \quad (20)$$

where SS and EP denote safeguard subject and endpoint, respectively. Accordingly, 3 types of DF for each ODS were obtained, i.e. the DALY basis for human health, the NPP basis for primary productivity, and the money basis for social assets. However, biodiversity, the remaining safeguard subject of LIME, was excluded from the impact category of ozone depletion.

Table 3: The damage function of ozone depletion for 13 ODS species with direct calculation

ODS [a]	Human health (DALY kg^{-1} yr)				Primary productivity (kg kg^{-1} yr)		
	Damage function			DF	Damage function		DF
	Skin cancer		Cataract		Terrestrial [c]	Aquatic [d]	
	MM	BCC+SCC					
CFC-11	1.33e-4 [b]	4.58e-4	7.54e-4	1.34e-3	4.41e+0	2.85e+2	2.90e+2
CFC-12	1.40e-4	4.79e-4	7.89e-4	1.41e-3	4.61e+0	2.99e+2	3.03e+2
CFC-113	1.43e-4	4.90e-4	8.07e-4	1.44e-3	4.72e+0	3.05e+2	3.10e+2
Halon-1211	3.36e-4	1.15e-3	1.89e-3	3.38e-3	1.11e+1	7.29e+2	7.41e+2
Halon-1301	1.96e-3	6.71e-3	1.10e-2	1.97e-2	6.48e+1	4.23e+3	4.30e+3
HCFC-22	5.37e-6	1.84e-5	3.03e-5	5.41e-5	1.77e-1	1.15e+1	1.16e+1
HCFC-123	3.46e-7	1.19e-6	1.95e-6	3.49e-6	1.14e-2	7.39e-1	7.51e-1
HCFC-124	2.06e-6	7.07e-6	1.16e-5	2.08e-5	6.80e-2	4.40e+0	4.47e+0
HCFC-141b	1.19e-5	4.07e-5	6.70e-5	1.20e-4	3.92e-1	2.53e+1	2.57e+1
HCFC-142b	8.17e-6	2.80e-5	4.62e-5	8.24e-5	2.70e-1	1.74e+1	1.77e+1
CCl_4	1.29e-4	4.41e-4	7.26e-4	1.30e-3	4.25e+0	2.75e+2	2.79e+2
1,1,1-TCE	9.06e-6	3.11e-5	5.12e-5	9.13e-5	2.99e-1	1.94e+1	1.97e+1
CH_3Br	6.36e-7	2.24e-6	3.66e-6	6.53e-6	2.17e-2	1.43e+0	1.45e+0

[a] Damage functions of the other 83 species regulated by the Montreal Protocol, not shown here, were determined indirectly.
[b] For instance, 1.33e-4 denotes 1.33×10^{-4}.
[c] Damage function for terrestrial NPP covers only coniferous forests excluding alpine-coniferous forests.
[d] Damage function for aquatic NPP covers only high latitudes, i.e. north of lat. 50°N or south of lat. 50°S.

ODS	Social assets (yen kg^{-1} yr)					
	Damage function					DF
	Crop production				Timber production	
	Soy	Rice	Peas	Mustard		
CFC-11	2.68e+0	3.15e+0	1.93e+0	4.70e-3	8.25e+1	9.03e+1
CFC-12	2.81e+0	3.30e+0	2.02e+0	4.92e-3	8.64e+1	9.45e+1
CFC-113	2.88e+0	3.38e+0	2.07e+0	5.03e-3	8.84e+1	9.67e+1
Halon-1211	6.75e+0	7.91e+0	4.86e+0	1.18e-2	2.09e+2	2.28e+2
Halon-1301	3.93e+1	4.61e+1	2.83e+1	6.89e-2	1.21e+3	1.33e+3
HCFC-22	1.08e-1	1.27e-1	7.77e-2	1.89e-4	3.32e+0	3.63e+0
HCFC-123	6.96e-3	8.18e-3	5.00e-3	1.22e-5	2.14e-1	2.34e-1
HCFC-124	4.15e-2	4.87e-2	2.98e-2	7.25e-5	1.27e+0	1.39e+0
HCFC-141b	2.39e-1	2.80e-1	1.72e-1	4.18e-4	7.34e+0	8.03e+0
HCFC-142b	1.64e-1	1.93e-1	1.18e-1	2.88e-4	5.05e+0	5.53e+0
CCl_4	2.59e+0	3.04e+0	1.86e+0	4.53e-3	7.95e+1	8.70e+1
1,1,1-TCE	1.82e-1	2.14e-1	1.31e-1	3.19e-4	5.60e+0	6.13e+0
CH_3Br	1.31e-2	1.53e-2	9.43e-3	2.30e-5	4.06e-1	4.44e-1

2.2 Damage indicator of stratospheric ozone depletion

The total damage for each safeguard subject induced by the ozone depletion, i.e. the damage indicator *DI* of ozone depletion, due to an alternative or an activity can be evaluated when its inventory for ODS emission was given.

$$DI(X, SS) = \sum_{EP} Inv(X) \cdot DF(X, SS) \quad (21)$$

where $Inv(X)$ denotes an inventory of X.

The damage indicator is what determined for each safeguard subject that individually has a different unit. LIME also developed a set of weighting factors based on conjoint analysis (Itsubo et al. 2004) that enables one to acquire an integrated indicator involving the all safeguard subjects, a so-called single index.

3 Discussion

3.1 Concept of damage

One of the difficult problems regarding impact assessment is the time delay between cause and effect. It takes a long time that such a low level of increasing UVB radiation exposure induces adverse effects on endpoints; it particularly becomes several decades for human health and terrestrial vegetation. The concept of damage, therefore, is interpreted

here that all of the future effects due to an additional emission at a certain time point is evaluated just at the time point of emission with the assumption of a constant baseline. Namely, the effects of any direct discount of the future impact, changes in adaptation ability against the impact, and changes in the baseline impact, were excluded from the damage function.

3.2 Parameter representativeness

3.2.1 UVB transfer

The effect of clouds that scatter and absorb ultraviolet radiation was excluded from the damage function of ozone depletion. The effect of the surface albedo that affects the ratio of reflection of ultraviolet radiation was also excluded; e.g. ice and snow surfaces have a large reflection ratio that increases the net exposure of UVB in white lands. In this context, an amount of UVB in the damage function is a semi-quantitative value. However, the effect of the difference from the actual exposure could be weakened by introducing the damage function indirectly, thus correlating the information of damage owing to epidemiological studies or experiments to indexical UVB values, instead of directly converting an indexical UVB value into some potential damage.

As shown in Fig. 4, the relationship between additional ODS emission and UVB increase at the earth's surface keeps its linearity up to the level of several hundreds of Gg emission per year. It is sufficient enough for practical usage, because an assessment deals with the order of kg per year emission of ODS.

The effect of altitude on the UVB attenuation was also excluded from the damage function except the process to determine F_{SCI} for skin cancer shown in section 1.6.1.

The atmospheric lifetime of certain ODS is dynamically alterable owing to the changes in such a burden in the atmosphere. The values of atmospheric lifetime were according to WMO (1999) here. The values correspond to the estimates with the assumption of the constant of atmospheric burden.

3.2.2 Human health

The relationship between UVB exposure and health impact should be found as the response to a marginal increase of UVB exposure at the same place. However, it is very difficult to obtain such information regarding human health in particular. The damage function of ozone depletion, therefore, chose the method that substituted the differences in UVB exposure and incidence between regions instead. This comprises the long-term adaptation of inhabitants against UVB exposure that leads to underestimate the response to a marginal increase of UVB exposure.

There were two sources of information regarding skin cancer incidence of white race. LIME adapted the F_{SCI} derived from the Australian epidemiological study (Armstrong 1993) that was several ten-fold larger than that derived from the world epidemiological study (Ferlay et al. 1997). The reasons for the decision were, (1) it was assumed that the skin cancer incidence of the white Australian mainly composed of immigrants resembled the response of skin cancer incidence to rapid increases of UVB exposure, (2) the better correlation of the skin cancer incidence of the white Australian to annual Ery-UVB was found, and (3) more detailed classification of skin cancer, MM, BCC, and SCC was available. Although BCC and SCC were finally aggregated into non-melanoma skin cancer; it was to be made consistent with the limited classification of skin cancer for the yellow and black races.

3.2.3 Primary productivity

The damage function of ozone depletion covered only coniferous forests in the aspect of terrestrial primary productivity due to the data availability. However, the increase of UVB exposure induced by ozone depletion notably appears in high latitudes where coniferous forests dominate. Hence, the present damage function can be evaluated that involves the most susceptible vegetation against ozone depletion.

For aquatic NPP, LIME employed the way that deleted D, chlorophyll-a density, by using the function of D to express k, extinction coefficient (Taguchi et al. 1994). However, it is possible to overestimate damage when an actual value of D is low and inapplicable to the relationship between D and k. LIME approves the way, because the productivity of aquatic zones in high latitudes is relatively high, namely the value of D is relatively high.

3.2.4 Social assets

As to crop production, other important crops in the aspects of production largeness, e.g. main cereals such as wheat, burley, and maize, other crops such as potatoes, sweet potatoes, and tomatoes should be quantitatively evaluated in LCIA. Quantitative data regarding the relationship of yield to UVB exposure for these crops are fundamentally required. Meanwhile, there are large differences in producer cost between regions. Ideally, it is desirable that the summation of the producer costs over the world was done after the conversion of the producer cost in each country into the currency of the objective country, i.e. Japan here. However, it was hardly possible because of the sharp fluctuations in exchange rates. Hence, the conversion into yen was done by uniformly multiplying the production in the world by the producer cost in Japan; it might overestimate the damage due to the highness of prices in Japan.

As to timber production, the assumption regarding NPP damage as timber production damage implies that both are sustainable under the steady state condition. Moreover, the same problem as crop production exists in the aspect of producer cost.

3.3 Comparison with other estimates

UNEP (1994) shows that the 1% decrease in stratospheric ozone will increase the incidence of non-melanoma skin cancer by 2%. The similar estimation using the revised damage function showed a 7% increase in the world incidence of non-

melanoma skin cancer corresponding to the uniformly 1% decrease in total ozone for each season and each latitudinal zone. The previous estimation (Hayashi et al. 2000) showed the 0.7% increase under the same condition; it is a tenth part of the present estimation. That is because the relationship of skin cancer incidence in the white race to an increase of UVB was revised to be more serious in this study.

UNEP (1994) also shows that the 1% decrease in total ozone will increase the incidence of cataract by 0.6–0.8%. The similar estimation using the revised damage function showed a 0.5% increase in the world incidence of cataract corresponding to the uniformly 1% decrease in total ozone for each season and each latitudinal zone; that was at the same level as the estimation shown in UNEP (1994).

The Eco-indicator 99 (Goedkoop and Spriensma 2000) is another LCIA framework with the endpoint approach toward the impact category of ozone depletion, however, that only aims at the aspects of human health, skin cancer and cataract, regarding the endpoints of ozone depletion. **Table 4** compares the damage factors of the Eco-indicator 99 with the damage function of LIME. The values of DALY per case are basically the same between the two studies. Furthermore, the target diseases for human health were also the same. Therefore, the differences between two studies are ascribed to the differences in the part of UVB transfer and the part of dose-response relationship. It can be said that the two studies well agree with each other except for several ODS species. The hundred-fold difference in CH_3Br (see Table 4) was due to the revision of its atmospheric life time to be shorter, 1.3 year (WMO 1995) to 0.7 year (WMO 1999). In the previous paper (Hayashi et al. 2000), the values of DF of LIME were several percents of DF of the Eco-indicator 99. This result was brought about by the following reasons, (1) the previous study excluded cataracts that account for half of the DF (see Table 3), and (2) the relationship of skin cancer incidence to UVB exposure for the white race was revised to be more severe in this study.

Table 4: Comparison of damage function of ozone depletion between LIME and Eco-indicator 99

ODS	DF of Human health (DALY kg^{-1} yr)		
	LIME A	EI 99 [c] B	B/A
CFC-11 [a]	1.34e-3	1.05e-3	0.78
CFC-113 [a]	1.44e-3	9.48e-4	0.66
CFC-114	1.34e-3	8.95e-4	0.67
CFC-115	8.07e-4	4.21e-4	0.52
CFC-12 [a]	1.41e-3	8.63e-4	0.61
Halon-1201 [b]	–	1.47e-3	–
Halon-1202 [b]	–	1.32e-3	–
Halon-1211 [a]	3.38e-3	5.37e-3	1.6
Halon-1301 [a]	1.97e-2	1.26e-2	0.64
Halon-2311 [b]	–	1.47e-4	–
Halon-2401 [b]	–	2.63e-4	–
Halon-2402	6.76e-3	7.37e-3	1.1
HCFC-123 [a]	3.49e-6	1.47e-5	4.2
HCFC-124 [a]	2.08e-5	3.16e-5	1.5
HCFC-141b [a]	1.20e-4	1.05e-4	0.88
HCFC-142b [a]	8.24e-5	5.26e-5	0.64
HCFC-22 [a]	5.41e-5	4.21e-5	0.78
HCFC-225ca	2.46e-5	2.11e-5	0.86
HCFC-225cb	3.25e-5	2.11e-5	0.65
CCl_4 [a]	1.30e-3	1.26e-3	0.97
1,1,1-TCE [a]	9.13e-5	1.26e-4	1.4
CH_3Cl	–	2.11e-5	–
CH_3Br [a]	6.53e-6	6.74e-4	100
Other ODSs	available for 78 species	–	–

[a] ODSs with direct calculation of the damage function for LIME.
[b] ODSs not regulated by the Montreal Protocol and excluded from LIME.
[c] Eco-indicator 99 (Goedkoop and Spriensma 2000). The values correspond to the damage factors of egalitarian and hierarchist.

4 Conclusion

The present damage function of ozone depletion has two advantages in covering all ODSs regulated by the Montreal Protocol and covering important endpoints to any extent possible. However, to stretch a point, it should be noted that immunosuppression, perhaps an important endpoint of human health, is desirable to be evaluated as far as quantitative information is available. We consider that the present damage function is sufficient enough for the purpose of LCIA.

Uncertainty of damage function is also important to be elucidated. Preliminary studies have begun for the damage function of ozone depletion (Itsubo et al. 2002). However, it is a serious matter to collect all the quantitative information on the uncertainty of relevant parameters. Further analysis is required to comprehensively evaluate the uncertainty of the damage function.

Acknowledgements. This research was funded by a grant from the New Energy and Industrial Technology Development Organization of Japan. The authors would like to express our appreciation to Dr. Masaji Ono, National Institute of Environmental Studies of Japan, for his helpful cooperation in estimating the damage function of skin cancer and cataract.

References

Armstrong BK (1993): How Much Melanoma Is Caused by Sun Exposure? Melanoma Res 3, 395–401

Behrenfeld BJ, Chapman JW, Hardy JT, Lee H II (1993a): Is There a Common Response to Ultraviolet-B Radiation by Marine Phytoplankton? Marine Ecology Progress Series, 102, 59–68

Behrenfeld BJ, Hardy JT, Gucinsiki H, Hanneman A, Lee H II, Wones A (1993b): Effect of Ultraviolet-B on Primary Production along Transects in the South Ocean. Marine Environ Res 35, 349–363

Caldwell MM (1971): Solar Ultraviolet Radiation and the Growth and Development of Higher Plants. In: Photobiology (Ed Giese AC) 6, Academic Press, New York, 131–177

CIE (International Commission on Illumination) (1987): A Reference Action Spectrum for Ultraviolet Induced Erythema in Human Skin. CIE Journal 6, 17–22

Daniel JS, Solomon S, Albritton DL (1995): On the Evaluation of Halocarbon Radiative Forcing and Global Warming Potentials. J Geophys Res 100, 1271–1285

Dourmishev AL, Popova LI, Dourmishev LA (1997): Basal and Squamous Cell Carcinoma: Sex, Age and Location Distribution. In: Skin Cancer and UV Radiation (Eds Altmeyer et al.), Springer-Verlag Berlin, 540–546

FAO (Food and Agriculture Organization) (2000) Agricultural Production (Crops Primary). FAOSTAT, CD-ROM

Ferlay J, Black RJ, Whelan SL, Parkin DM (eds) (1997): CI5VII Electronic Database of Cancer Incidence in Five Continents. International Agency for Research on Cancer, Lyon

Goedkoop M, Spriensma R (2000): The Eco-indicator 99, A Damage Oriented Method for Life Cycle Impact Assessment, Methodology Report 2nd Edition. PRé Consultants, Amersfoort, 132 pp

GSFC (Goddard Space Flight Center) (2000): SeaWiFS Project Home Page. NASA

Hayashi K, Itsubo N, Inaba A (2000): Development of Damage Function for Stratospheric Ozone Layer Depletion – A Tool Towards to the Improvement of the Quality of Life Cycle Impact Assessment. Int J LCA 5, 265–272

Hayashi K, Nakagawa A, Itsubo N, Inaba A (2002): Assessment of Impacts Due to Additional Emission of Ozone Depleting Substances. Proceedings of the 5th International Conference on EcoBalance 33–36

Houghton JT (1986): The Physics of Atmospheres: Second Edition. Cambridge University Press, Cambridge, 271 pp

Itsubo N, Hayashi K, Inaba A (2002): Uncertainty Analysis for Impact Assessment Based on Endpoint Modeling. Abstracts of the SETAC Europe 12th Annual Meeting, Vienna, p 47

Itsubo N, Inaba A (2003): A New LCIA Method: LIME has been completed. Int J LCA 8, 305

Itsubo N, Sakagami M, Washida T, Kokubu K, Inaba A (2004): Weighting Across Safeguard Subjects for LCIA through the Application of Conjoint Analysis. Int J LCA 9, 196–205

Jendritzky G, Staiger H, Bucher K (1997): UV Prognosis and UV Index Services in Europe. In: Skin Cancer and UV Radiation (eds Altmeyer et al.), Springer-Verlag, Berlin, 37–49

JMA (Japan Meteorological Agency) (1998): Annual Report on Monitoring the Ozone Layer (CD-ROM). 8, Tokyo

Kaye JA, Penkett SA, Ormond FM (eds) (1994): Report on Concentration, Lifetime, and Trends of CFCs, Halons, and Related Species. NASA Reference Publication, 1339, NASA, 247 pp

Kossuth SV, Biggs RH (1981): Ultraviolet-B Radiation Effects on Early Seedling Growth of Pinaceae Species. Can J For Res 11, 243–248

Krupa SV, Kickert RN (1989): The Greenhouse Effect, Impacts of Ultraviolet-B (UVB), Carbon Dioxide (CO_2), and Ozone (O_3) on Vegetation. Environ Pollut 61, 263–293

Liou KN (2002): An Introduction to Atmospheric Radiation 2nd Edition. International Geophysics Series 84, Academic Press, 583 pp

MAFF (Ministry of Agriculture, Forestry and Fisheries of Japan) (2002a): 76th Statistical Yearbook of Ministry of Agriculture. Forestry and Fisheries. MAFF (in Japanese)

MAFF (2002b): Annual Report of Timber Supply-Demand in 2000. MAFF (in Japanese)

Matthews E (1983): Global Vegetation and Land Use: New High Resolution Data Bases for Climate Studies. J Clim Appl Meteorol 22, 474–487

McPeter R, Beach E (Eds) (1996): TOMS Version 7 O_3 Gridded Data: 1978–1993 (CD-ROM). Goddard Space Flight Center, NASA

Murray CJL, Lopez AD (1996): The Global Burden of Disease: A Comprehensive Assessment of Mortality and Disability from Diseases, Injuries, and Risk Factors in 1990 and Projected to 2020. Global Burden of Disease and Injury, 1, Harvard University Press, 990 pp

Naidu SL, Sullivan JH, Teramura AH, DeLucia EH (1993): The Effects of Ultraviolet-B Radiation on Photosynthesis of Different Aged Needles in Field-Grown Loblolly Pine. Tree Physiol 12, 151–162

Nielsen SE (1960): Productivity of the Oceans. Ann Rev Plant Physiol 11, 341–362

Ono M (2002): Studies on Ultraviolet Radiation and Health Effects: Ocular Exposure to Ultraviolet Radiation. In: Progress in Lens and Cataract Research (eds Hockwin et al.), Developments in Ophthalmology 35, Karger, Basel, 32–39

Redfield AC, Ketchum BH, Richards FA (1963): The Influence of Organisms on the Composition of Sea Water. In: The Sea Vol. 2 (ed Hill), Interscience, London, 26–77

Sasaki M, Takeshita S, Sugiura M, Sudo N, Miyake Y, Furusawa Y, Sakata T (1993): Ground-Based Observation of Biologically Active Solar Ultraviolet-B Irradiance at 35°N Latitude in Japan. J Geomag Geoelectr 45, 473–486

Sasaki K, Sasaki H, Kojima M, Shui YB, Hockwin O, Jonasson F, Cheng HM, Ono M, Katoh N (1999): Epidemiological Studies on UV-Related Cataract in Climatically Different Countries. J Epidemiology 9, S-33–S-38

Solomon S, Albritton DL (1992): Time-dependent Ozone Depletion Potentials for Short- and Long-term Forecasts. Nature 357, 35–37

Sullivan JH, Teramura AH (1992): The Effects of Ultraviolet-B Radiation on Loblolly Pine. 2. Growth of Field-Grown Seedlings. Trees Structure and Function 6, 115–120

Taguchi S, Saito H, Kasai H (1993): Characteristics of ultraviolet radiation penetration in the sea and its effects on marine phytoplankton community in the western subarctic Pacific. Proceedings of the 13th UOEH International Symposium on Impact of Increased UV-B Exposure on Human Health and Ecosystem, 251–264

UN (United Nations) (1998): Sex and Age Annual 1950–2050 (The 1998 Revision). United Nations Secretariat

UNEP (United Nations Environmental Programme) (1998): Environmental Effects of Ozone Depletion: 1998 Assessment, UNEP, Nairobi

Whittaker RH (1975): Communities and Ecosystems 2nd Edition. Macmillan Company, New York

WMO (World Meteorological Organization) (1995): Scientific Assessment of Ozone Depletion. WMO Report, 37

WMO (1999): Scientific Assessment of Ozone Depletion: 1998 Assessment. WMO Report, 44

Received: July 20th, 2004
Accepted: November 10th, 2004
OnlineFirst: November 10th, 2004